REVISION 2

MOLYBDENITE-BEARING VUGS IN MICROGRANITE IN THE PREISSAC PLUTON, QUÉBEC, CANADA: RELICTS OF AQUEOUS FLUID POCKETS?

THOMAS MULJA[1] AND ANTHONY E. WILLIAMS-JONES

Department of Earth and Planetary Sciences, McGillUniversity,

3450 University St., Montréal, Qc., CanadaH3A 0E8

TEXT

Resubmitted to American Mineralogist
Manuscript # 8770R

21 March, 2023

[1]Present address:3709 Rutherford Cres., North Vancouver, B.C. Canada V7N 2C6.
Tel: +16049805897
Corresponding author: mulja@protonmail.com

ABSTRACT

Field, petrochemical, and stable isotope data from peraluminous microgranite dikes and their molybdenite-bearing vugs in the Archean Preissac-Lacorne batholith, Québec, provide evidence for the transport and deposition of molybdenite by an aqueous fluid that exsolved from a felsic magma. A model is proposed in which the microgranite-forming liquid fractionated from a magma that was parental to and intruded less evolved muscovite monzogranite. Fluid saturation is interpreted to have occurred immediately prior to emplacement, allowing sufficient time for small spherical pockets of fluid to form and rise through the liquid, but insufficient time for them to leave the system. These fluid pockets scavenged molybdenum and other components during their migration, but were frozen *in situ* to form molybdenite-bearing vugs as a result of the quenching of the magma. We therefore conclude that the vugs are relicts of the exsolved fluid pockets, and that the molybdenite in them reflects the concentration of molybdenum in the fluid, estimated from volumetric relationships to have reached ~7800 parts per million (ppm).

Keywords: Molybdenum mineralization, miarolitic cavity, volatile exsolution, monzogranite, Québec.

INTRODUCTION

Geological, mineralogical, and isotopic studies of granite-related molybdenum deposits have established that Mo concentrates in the volatile-rich residual melt of a crystallizing magma before being partitioned into an exsolving fluid from which molybdenite eventually precipitates (e.g., Westra and Keith, 1981; Carten et al. 1988; Stein, 1988; Hannah et al., 1988; Audétat, 2010; Greany et al., 2018; Chang et al., 2020). Moreover, fluid and melt inclusion studies by

Cline and Bodnar (1994), Ross et al. (2002), and Audétat and Li (2017 and references therein) have shown that there is little or no contribution from meteoric waters to the composition of the aqueous phase. The magmatic fluid is considered to be released during degassing of the magma as bubbles of supercritical fluid that migrate in buoyant plumes toward a zone of volatile accumulation or percolation that eventually becomes the focus of fluid pressure-induced fracturing of the overlying rock and intense alteration and mineralization (Whitney, 1975; Burnham, 1979; Candela, 1991; Larsen et al., 2004).

Physical evidence for the above processes in granite-related Mo deposits and other types of intrusion-related metallic mineral deposits is rare. Although miarolitic cavities in granitic rocks are widely considered to be the products of fluids exsolved from volatile-saturated silicate melts (Candela, 1997; King and White, 2003; Peretyazhko et al., 2005), they seldom contain metallic minerals that are economically exploited. Such cavities are known to occur in Mo-mineralized granites, for example in the Allebuoda, Munka and Kåtaberget granites in Sweden (Öhlander et al., 1989), several granitic complexes in Australia (Candela and Blevin, 1995), the Treasure Mountain granite in Colorado, the Drammen and Glitrevann granites in Norway (Lerchbaumer and Audétat, 2013) and the Torres del Paine granites in Chile (Kaufmann et al., 2021). To our knowledge, however, only miarolitic cavities in the Glitrevann and Torres del Paine granites have been reported to contain molybdenite. In the case of the Glitrevann granite, there is no published information on the miarolitic cavities other than that they occur in the aplogranite zone of the intrusion and contain molydenite, pyrite, quartz, and alkali feldspar (Schonwandt, 1988). At Torres de Paine, the isolated miarolitic cavities range from a few millimeters up to 1 meter in diameter and are interpreted to represent late stage exsolved

magmatic hydrothermal fluids that were preserved as "bubbles" in the solidifying magma (Kaufmann et al. 2021). The contained minerals are therefore considered to have precipitated from the cavity-forming magmatic-hydrothermal fluid (Kaufmann et al. 2021). One of these cavities of unmentioned size was reported to contain "free-grown" molybdenite in the "loose cavity material" that comprises quartz, plagioclase, amphibole, titanite, and epidote (Kaufmann et al. 2021).

In 1990, one of us (AEW-J) noticed numerous isolated molybdenite-bearing vugs or miarolitic cavities in previously undescribed muscovite-garnet microgranite dikes in the Preissac pluton of the Archean Preissac-Lacorne batholith, Québec (Fig. 1A). This pluton hosts the former Preissac and Cadillac molybdenum mines, which had a combined total reserve of approximately 6.7 million tons of ore grading 0.2 wt.% Mo (Kirkham et al., 1982), making them among the largest Mo deposits in Canada. The vugs potentially provide field evidence for Mo transport by, and deposition from, orthomagmatic fluids that had been released directly from a silicate liquid and subsequently precipitated primary molybdenite crystals. In this communication, we use data from the field, petrography, mineral chemistry, whole-rock composition, and oxygen and sulfur isotopes to explore the origin of the vug-hosted molybdenite in the Preissac microgranite dikes. Additionally, we use simple numerical modeling to predict the concentration of the Mo in the fluid and compare this concentration with data from experiments on the solubility of Mo in hydrothermal fluids.

GEOLOGY AND PETROLOGY OF THE MICROGRANITE

The molybdenite-bearing microgranite dikes occur in the center of the Archean Preissac

pluton (2681–2660 Ma; Ducharme et al., 1997), a monzogranite comprising a narrow marginal northern biotite facies, an eastern two-mica facies, and a western muscovite facies (Fig. 1B). The former underground Preissac Mo mine is located approximately 1 km to the northwest of the microgranite and the exhausted Cadillac open-pit Mo mine about 2 km to the southwest. Ore-bearing quartz veins at both sites occur within muscovite granite at its contact with basaltic rocks (Watt, 1967; Taner et al., 1998), and consist of molybdenite rosettes intergrown with coarse-grained muscovite and pink K-feldspar. Samples of ore collected from the muck piles in the Preissac mine show that muscovite granite possesses textural and mineralogical features similar to those of the main body of the muscovite monzogranite. The microgranite dikes are up to four-meters wide, occur within the muscovite monzogranite, and cut quartz ± molybdenite veins and barren granitic pegmatite pods (Fig. 1C). These spatial relationships indicate that the Mo-bearing quartz veins likely originated from fluids released by the magma that crystallized the host muscovite monzogranite. This fluid is also interpreted to have formed the Preissac quartz vein Mo deposit. The microgranite dikes appear to be vertical and strike randomly, although the larger bodies trend NE-SW and E-W. The contact between the microgranite and the muscovite monzogranite is sharp, and there is no evidence of chilled margins. Microscopically, the contact is marked by epitaxial intergrowths of the feldspars and interlocking of crystals. Mulja et al. (1995a) estimated that the Preissac pluton was emplaced at a depth of about 8-9 km (or about 3.5 kbar) and crystallized at temperatures between 650° and 750° C.

The petrology and geochemistry of the microgranite were discussed briefly in Mulja et al. (1995a, b), and are elaborated on in this paper. Here we also present previously unpublished data on the compositions of the silicate minerals in the microgranite, the vugs, and the former Mo-

bearing vein ore. A CAMECA electron microprobe at McGill University was used to determine the compositions of the minerals under the following operating conditions: 15–20 Kv acceleration voltage, 8–20 nA current beam, focus to a 30μm beam diameter, and a 25–75 second counting time. Mineral standards were used for calibration. These were: albite (Na), orthoclase (Al, K, Si), diopside (Ca, Mg), magnetite (Fe), spessartine (Mn, Si, Al in garnet analyses), fluorite (F), molybdenite (Mo), pure metal (U), and synthetic MnTi (Mn, Ti), pyrrhotite (S, Fe), and columbite-tantalite ($MnNb_2O_6$ and Ta_2O_5 for Mn, Nb and Ta). The data reduction was accomplished with the full PAP correction procedures of Pouchou and Pichoir (1985). Two pulverized samples of microgranite adjacent to the molybdenite-bearing vugs were analyzed by X-ray diffraction (powder method) with a Rigaku XRD instrument at McGill University; the conditions were: a 40 mA current, a 160 kV voltage, a 2°to 60°Θ scan interval, a step width and time of 0.05° and 0.3 seconds, respectively and a 10° per minute scan speed. The diffractograms were evaluated using JADE software. Mulja et al. (1995b) reported the major and trace element concentrations of the microgranite, which were determined with X-ray fluorescence spectrometric analyses at McGill University; the rare-earth element concentrations were determined by instrumental neutron activation analyses at the Université de Montréal and by inductively coupled plasma mass spectrometry (ICP-MS) at Memorial University of Newfoundland.

The microgranite is fine-grained (~ 1 mm diameter crystals), and consists mainly of interlocking crystals of quartz (31%), K-feldspar (29%) and plagioclase (32%), and minor muscovite (4%) and garnet (3%) (Fig. 2). Subhedral to euhedral plagioclase crystals up to 1.5 mm in diameter display polysynthetic albite twinning and are unzoned to weakly zoned. They

have a composition from An_2 to An_5 and a median composition of An_3 (Table 1). Potassium feldspar crystals are generally smaller than the plagioclase crystals (1 mm in diameter on average), exhibit tartan twinning, and are microperthitic. However, some K-feldspar and quartz crystals are larger (1.5–2mm) than those of plagioclase, imparting a subtle porphyritic appearance to the rock. Regardless of its mode of occurrence, the composition of K-feldspar varies from $Or_{94\ to}\ Or_{98}$ with a median composition of Or_{96}, and the exsolved plagioclase is albitic (An_{0-2}). Approximately 10% of the feldspar grains is turbid and encloses minute sericite; a feature that signals incipient alteration.

Muscovite occurs as euhedral to subhedral flakes (1 mm), many of which are similar in size to those of other primary silicate minerals (Fig. 2). This size similarity and the morphology of the muscovite suggest strongly that muscovite crystallized contemporaneously with the other silicate minerals. The muscovite is aluminous with ΣAl values averaging 5.1 (4.98–5.36) a.p.f.u (atom per formula unit) and has relatively low concentrations of M^{2+} ions (0.54–0.84 a.p.f.u) (Table 1). The analyzed muscovite crystals are located at varying distances from the vugs but do not abut them. On the ternary ΣAl-Si-M^{2+} diagram of Monier and Robert (1986), the average composition of muscovite from the microgranite plots near the muscovite end member and is within the 500° and 550° C isotherms (Fig. 3). This temperature range is lower than that for the muscovite monzogranite (see above). Garnet, which comprises between 1 and 2 vol. % of the rock, is mostly euhedral and disseminated throughout the microgranite. Its composition is dominated by the spessartine (Sp_{55-62}, averaging Sp_{59}) and almandine (Alm_{37-42}, averaging Alm_{38}) components, with much lesser proportions of the andradite (< 2 mol.%) and pyrope (< 1.5 mol.%) components (Table 1). Individual garnet crystals are unzoned and their compositions

do not vary with distance from the vugs. The ubiquity, euhedral habit and consistent composition of the garnet point to an igneous origin as is the case for similar garnet in other leucogranites (see Villaros et al., 2009 and references therein). Thus, we conclude that the garnet formed early during the crystallization of the microgranite. The accessory phases comprise ferrocolumbite ($Fe_{0.5}Mn_{0.5}Nb_{1.9}Ta_{0.1}O_5$), zircon, uraninite, sphalerite, and pyrite (Mulja et al.,1995a).

Geochemically, the microgranite is highly siliceous, moderately peraluminous (A/CNK = 1.2), and sodic (Na/K = 1.2) (Table 2). Its Ba, Sr, Zr and Th contents are lower than those of the muscovite monzogranite which it intruded, whereas its Rb, Nb, Y and Cs contents are higher. The Mo content of the microgranite (devoid of molybdenite) is 0.35 ppm, and is lower than that of typical granite, which varies from 0.9 to 2.7 ppm and averages 1.8 ppm (Wedepohl, 1969) and that of the upper continental crust, which ranges from 0.78 to 1.5 ppm and averages 1.1 ppm (Wedepohl, 1995; Rudnick and Gao, 2003). Nonetheless, it is within the range of Mo contents of some leucogranites (0.26 to 0.84 ppm, Greaney et al., 2018); others, notably, highly evolved peraluminous molybdenite-bearing granitic plutons have been reported to contain up to 300 ppm Mo (Saleh, 2007). The sum of the rare-earth element contents is 17.2 ppm, and the chondrite-normalized REE profile shows a strong depletion in LREE, a large Eu negative anomaly and a slight HREE enrichment (Fig. 4A). These trace and rare earth element distributions, as pointed out by Mulja et al. (1995b), represent the end stage of fractional crystallization of a granitic magma that produced the monzogranite variants, i.e., the microgranite is the most evolved monzogranitic phase, not only in the Preissac pluton, but in the entire Preissac-Lacorne batholith (Fig. 4B), in which each pluton shows a similar mineralogical variation. Indeed, on the basis of LREE geochemistry, the microgranite is even more differentiated than an aplite from the

Lacorne pluton, or the highly evolved Honey Comb Hills rhyolite in Utah, which is regarded to be the extrusive equivalent of granitic pegmatite (Congdon and Nash, 1991). Furthermore, comparative trace element and REE data show that the microgranite is more evolved than other Mo ore-forming granites of peraluminous to peralkaline affinity (Fig. 5). It is noteworthy, however, that thorium, a highly incompatible element, that is normally enriched during end-stage fractional crystallization, is more enriched in the less evolved, mildly peraluminous Mo associated granites of Central Sweden than in the Preissac microgranite (Fig. 5). The probable reason for this is that Th was removed from the Presissac magma by the prior fractionation of Th-bearing monazite during crystallization of the monzogranite, leaving the residual magma which solidified as the microgranite depleted in Th

NATURE OF THE MOLYBDENITE-BEARING VUGS IN THE MICROGRANITE DIKES

The molybdenite-bearing vugs occur in randomly distributed clusters, each of which contains up to ten vugs and covers an area of approximately four-square meters. These vugs are commonly spherical, measuring 0.75- to 1.5-cm across (Fig. 6A-B). Some vugs are shallower than others, indicating either that they have a different shape or that most of their upper part has been eroded. The microgranite in contact with the vugs is finer-grained than that distal from it, suggesting local rapid cooling relating to aqueous phase separation from the magma. Analyses of plagioclase, as well as of muscovite and K-feldspar, yielded no evidence of significant compositional variation with distance from the vugs or molybdenite disseminations (Table 1). Reddish-brown stains and boxwork-like relicts from oxidized pyrite are present in almost all the vugs and surround the disseminated molybdenite (Fig. 6B-C). Powder X-ray diffraction analyses did not indicate the presence of clay minerals, such as kaolinite orillite in and around the vugs.

The oxidation is thus attributed to weathering, as no other evidence of post-magmatic hydrothermal alteration was detected elsewhere in the dikes.

A typical vug may contain several rosettes of molybdenite (2-5 mm across) that occupy approximately 1 volume % of the vug and are tapered at the vug bottom (Fig. 6B). These molybdenite crystals are intergrown with muscovite, which constitutes part of the vug mineralogy (Fig. 6D). Euhedral crystals of pyrite (1 mm) generally occur in and near the vugs. In addition to the molybdenite in the vugs, molybdenite crystals in the same size range are sparsely disseminated in the microgranite. The chemical composition of the molybdenite and pyrite is stoichiometric. Muscovite intergrown with molybdenite in the vugs is compositionally similar to that around the host microgranite, and this composition overlaps that of muscovite away from the vugs (Table 1, Fig. 3). Moreover, compared to muscovite crystals from ore samples and along vein selvages, which clearly had a post-magmatic hydrothermal origin, muscovite in the vugs and microgranite is more aluminous and contains a smaller proportion of the celadonite component (X_{cel}: 0.15 versus 0.25). These comparisons support a conclusion that the vug muscovite is of magmatic origin.

OXYGEN AND SULFUR ISOTOPE ANALYSES

The oxygen isotopic composition of two microgranite samples was analyzed at the Université de Montréal with the BrF_5 method of extraction of Clayton and Mayeda (1963). Details of the analytical methods are given in Hoy (1993). The values of $\delta^{18}O$ are reported relative to Vienna SMOW (Standard Mean Ocean Water). Molybdenite separates for sulfur isotope analyses were hand-picked from two vugs and were cleaned in an ultrasonic bath for 25

minutes. Sulfur isotope analyses were conducted at the Isotope Laboratory of the University of Saskatchewan and the values of $\delta^{34}S$ reported relative to the Vienna Canyon Diablo troilite. The measured whole-rock $\delta^{18}O$ values of the microgranite are 8.7 and 8.9‰, and the $\delta^{34}S$ values of the molybdenite samples are −0.3 and −1.1‰.

DISCUSSION

Interpretation of field relations and petrochemical data

The microgranite dikes are enclosed within unaltered muscovite monzogranite and cut small quartz veins in the muscovite monzogranite, i.e., they were emplaced after cessation of local veining. The epitaxial relationships of the major silicate minerals along the contact between the microgranite and muscovite monzogranite point to their formation within incompletely crystallized felsic liquids (see Hibbard 1980; Hibbard and Watters, 1985). Additionally, the microperthititic texture of the K-feldspar of the microgranite is more likely a consequence of thermal adjustment than a widespread fluid-rock interaction that would have produced braided or coarse lamellae (Brown and Parson, 1989). Furthermore, sericitization of some of the feldspar crystals was probably a local phenomenon, and the absence of clay minerals in and around the vugs points to limited low-temperature fluid-rock interaction. This interpretation is supported by the whole rock $\delta^{18}O$ compositions of the microgranite dikes (8.7 and 8.8‰), which are similar to those of the muscovite monzogranite in the Preissac pluton (8.2 − 8.8‰; Mulja et al. 1995b), and have been interpreted to indicate that the rocks did not undergo significant interaction with meteoric water. Finally, the $\delta^{34}S$ values of the molybdenite samples, −0.3 and −1.1‰, are well within the range of −3 to +3‰ determined for granitic melts and of −3 to +7‰ estimated for magmatic hydrothermal fluids (see Ohmoto and Rye, 1979). These observations provide strong

evidence that magmatic processes dominated the development of the microgranite dikes and related molybdenum mineralization, and that post-magmatic hydrothermal alteration was negligible.

The magmatic processes mentioned above thus largely controlled the distribution of the REE in the microgranite (Fig. 4A). Mulja et al. (1995b) reported the presence of monazite and calcic plagioclase in the two-mica and muscovite monzogranites of the Preissac pluton. However, these minerals are absent from the microgranite, which explains its depleted LREE contents and strong negative Eu anomaly. By contrast, the garnet abundance is significantly higher than in the two-mica monzogranite, which may explain the enrichment in HREE. The progressive changes in REE_N and trace elements from the muscovite monzogranite to the microgranite (Fig. 4A) suggest that these intrusions are related by fractional crystallization. We propose that this process must also have been responsible for the formation of the microgranite-hosted vugs and the minerals contained therein. This proposal follows from the fact that fractional crystallization of relatively hydrous melts typically leads to the development of residual liquids that are rich in cavity-forming fluids (as shown by the presence of primary muscovite in the Preissac microgranite; also see Chakraborty and Upadhyay, 2020). Indeed, the upward growth of the molybdenite rosettes in the microgranite vugs resembles that of many minerals inside miarolitic cavities in granitic pegmatites and granites, which have been interpreted to be of magmatic origin and to have formed from fluids exsolved from water-saturated magmas (Taylor et al., 1979; Stern et al., 1986; Candela, 1997). Moreover, as demonstrated previously, the muscovite interleaved with the molybdenite is compositionally indistinguishable from liquidus muscovite in the host microgranite.

Although the oxidation state of the monzogranitic magma cannot be directly determined, it can be constrained as follows. At a crystallization temperature of 650°-500° C (Mulja et al., 1995a and Fig. 3 above), in the absence of pyrrthotite and the presence of pyrite, the microgranite magma would have had log fO_2 values from −20 to −12.5. These values are higher than those of many porphyry Mo deposits that range from −23 to −17.5 at 675° to 450° C (see Fig. 8 in Yang et al., 2014). Thus, the microgranite magma was relatively oxidized, and this inference is consistent with the conclusion of Blevin and Chappell (1992), Jian et al. (2015), and Shang et al. (2020) that a relatively oxidized magma is required to generate granite-hosted hydrothermal Mo deposits.

Vug formation

Miarolitic cavities or vugs in granitic rocks, as stated previously, develop as a result of exsolution of an aqueous phase from a crystallizing magma. This exsolution is most effectively triggered by decompression relative to crystallization (Whitney, 1989), which was the case for the Preissac microgranite, since it was emplaced as dikes, i.e., the magma was injected into fractures in the muscovite monzogranite. Shinohara and Kazahaya (1995) proposed that exsolved fluid bubbles ascend due to their buoyancy in narrow zones in a stagnant magma, or disseminate in a convecting magma. An analogy to the former is illustrated in Figure 7, which shows individual columns of vesicles (gasses or gas mixtures) in basaltic lava flows that terminate in a vesicle-rich zone parallel to the top of the flow. We speculate that the columns and vesicle-rich zone correspond, respectively, to the buoyant plumes of bubbles and the critical zone of volatile percolation envisaged by Candela (1991). In a convecting, volatile-rich magma, bubbles are dispersed and the paths to the zone of percolation are no longer evident. The molybdenite-

bearing vugs, which form randomly distributed clusters of vugs, could reflect this scenario. If, however, the vug clusters in the Preissac microgranite represent a slice through a bubble-rich zone fed by ascending bubble columns, then they could be evidence of the buoyant plume model of fluid release. The current exposure cannot resolve this issue, which would require a cross-sectional view of the dikes.

Molybdenum speciation in magmatic-hydrothermal systems

As a high-field strength element with a *Z/r* (atomic number over radius) value from 7.5 to 11, depending on its oxidation state, Mo is not readily incorporated in early crystallizing minerals and hence will concentrate in the residual magma during fractional crystallization. This effect would have been particularly pronounced in the Preissac pluton because the precursor of the highly evolved microgranite, namely the monzogranite, lacks minerals such as ilmenite, magnetite, and titanite, which might have acted as sinks for Mo during the above differentiation. In silicate melts, molybdenum dissolves predominantly as tetrahedral $\mathrm{Mo(VI)O_4^{2-}}$moieties, i.e., Mo is in its most oxidized form for a wide range of fO_2 conditions, although in the presence of H_2O or elevated concentrations of halogens, some Mo may occur as octahedrally co-ordinated $\mathrm{Mo(IV)O_6^{8-}}$ (Farges et al., 2006). Significantly, however, neither H_2O nor the halogens form stable complexes with molybdenum. By contrast, molybdenum forms relatively strong complexes with sulfur, e.g., species such as $\mathrm{Mo(VI)S_3^{2-}}$and $\mathrm{Mo(IV)S_3^{4-}}$, or at high fugacity of sulfur, $\mathrm{Mo(IV)S_4^{4-}}$ (Farges et al., 2006).

The Mo content of most peraluminous magmas is relatively low, commonly on the order of no more than a few ppm (e.g., Noble et al., 1984), despite the solubility of molybdenum in such magmas being much higher. For example, in a magma containing 1 mole% S (a moderately

high concentration of sulfur) the solubility of Mo is approximately 2,100 ppm at 750° C and 2,500 ppm at 800° C; above these concentrations, molybdenite will crystallize as a liquidus mineral (Ryabchikov et al., 1981; Štemprok, 1990). Highly evolved peraluminous granites that are genetically associated with the formation of aplite or pegmatite-hosted molybdenite deposits may have elevated molybdenum contents. This is the case for peraluminous plutons in the South Eastern desert of Egypt, for which Saleh (2007) has reported Mo concentrations of between 100 and 300 ppm. In the Preissac microgranite dikes, the Mo content, as indicated previously, is only 0.35 ppm. Such a low value is most plausibly interpreted to reflect the efficient scavenging of Mo from the magma by an exsolving hydrothermal fluid consistent with the occurrence of molybdenite-bearing vugs (Fig. 6). This deduction is supported by the observation of Audétat et al. (2011) that granitic rocks cogenetic with magmatic-hydrothermal Mo deposits have low Mo contents and with the related conclusion of Greaney et al. (2018) that, on average, granites are missing 60% of their expected Mo content. These studies attributed the deficit to the partitioningof Mo into an aqueous magmatic fluid and its expulsion from the cooling plutons.

When a magma saturates with and exsolves an aqueous fluid, the molybdenum generally partitions preferentially into this fluid in amounts that depend on salinity, fO_2, $f\ S_2$,pressure, temperature and the composition of the magma. Not surprisingly, therefore, experimental studies of the partitioning of molybdenum between fluid and granitic melt ($D_{Mo}^{f/m}$) have yielded a wide range of values, i.e., from 0.07 (Bai and van Groos, 1999) to 135 (Tattitch and Blundy, 2017). Most of these studies, however, have been for sulfur-free systems and few have considered the role of pressure in controlling $D_{Mo}^{f/m}$. An important exception is the study of Fang and Audétat

(2022). They reported $D_{Mo}^{f/m}$ values for slightly peraluminous, magnetite–pyrrhotite-pyrite buffered melts at 750° C that increase from 9 ± 2 at 160 MPa to 11 ± 4 at 200 MPa and 14 ± 2 MPa or 2.5 kbar, i.e., a magma with a composition similar to and oxygen fugacity marginally below those discussed above for the Preissac microgranite; the X_{NaCl} was 0.07. The only other study to consider sulfur in their experiments for comparable oxygen fugacity (NNO + 2) were those of Tattich and Blundy (2017). An expression reported by them for $D_{Mo}^{f/m}$as a function of X_{NaCl} and X_{H2O}, based on experiments conducted at 100 and 200 MPa and the same value of X_{NaCl} as that employed by Fang and Audétat (2022) yielded a $D_{Mo}^{f/m}$ value of 30.2; the value of X_{H2O} is that reported for a water-saturated felsic melt at 750° C, fO_2 = NNO + 1, and 140 MPa (Rutherford and Devine, 1988).

Fang and Audétat (2022) concluded, based on a set of complementary speciation experiments in sulfur-bearing, iron-free experiments, that Mo was present in their experiments dominantly as $NaHMoO_4$. Significantly, Shang et al. (2020), reached the same conclusion for lower temperature, and in experiments at 350 °C with solutions having a NaCl molality of ~ 2 (12 wt %), obtained dissolved Mo concentrations up to 4600 ppm, albeit at low pH.

Molybdenum concentration in the magmatic fluid

Based on our earlier description of the vugs in the Preissac microgranite and the consistency in the volumetric proportion of molybdenite from one vug to the next, it seems clear that the molybdenite presently in the vugs precipitated after the latter had formed as isolated cavities disconnected from the channels of fluid flow (Fig. 6C). Assuming this to be the case, it follows that the mass of molybdenite in a vug should provide a direct measure of the

concentration of molybdenum in the fluid, and a rare opportunity to quantify molybdenum transport in a natural system at or near magmatic conditions. As a typical vug (spherical) has a diameter of 1.5 cm and a typical molybdenite rosette (right cylinder) has a radius of 1.5 mm and a height of 0.5 mm, the volume of fluid would have been 1.77 ml, and the volume of molybdenite precipitated from this fluid would have been 0.0035 ml.

As shown in Figure 3, the muscovite in the microgranite crystallized at 500°–550° C and, as previously mentioned, the Preissac-Lacorne monzogranites were emplaced at a pressure of ~3.5 kbar. Hence, fluid exsolution from the microgranite magma occurred in or above this temperature range and the Mo-bearing vugs formed at a temperature of ≥ 550° C. At this 550° C and a pressure of 3.5 kbar, the molar volume of the fluid is estimated to have been 23.2 ml (from Table 4 in Anderko and Pitzer, 1993), assuming that the fluid was aqueous and contained 10 wt.% NaCl (a conservative estimate according to Webster, 1997). The mass of the fluid, therefore, would have been 0.0761 moles or 1.372 gm and the mass of Mo would have been 0.0107 gm. Based on these calculations, the concentration of Mo in the fluid is estimated to have been ~7,800 ppm. It should be noted that this value does not consider any shrinkage in the size of the vugs that almost certainly occurred during crystallization of the liquid and the true concentration could have been lower.

The concentration of Mo estimated for the vug-forming fluids is an order of magnitude higher than concentrations (up to 760 ppm) reported in the literature for fluid inclusions in porphyry deposits, for example, by Audétat and Pettke (2003). However, this does not necessarily mean that the concentration estimated in this study is unrealistic, particularly considering that the pressures of the porphyry fluids are considerably lower (< 1 kbar) than those

estimated for the emplacement of the microgranite (3.5 kbar). As mentioned above, Fang and Audétat (2022) reported a $D_{Mo}^{f/m}$ value of 14 ± 2 at 250 MPa or 2.5 kbar and 750° C for a melt with a composition and at conditions similar to that of the microgranite magma. Assuming a $D_{Mo}^{sf/m}$ value of 20 (to account for the higher pressure of emplacement of the microgranite magma) and an initial concentration of 300 ppm Mo in the magma (similar concentrations have been reported for highly evolved peraluminous granites by Saleh, 2007), this would correspond to a concentration in the fluid of 6,000 ppm, which is a little below that estimated for the Preissac microgranite vug-filling fluid (7,800 ppm). As also mentioned above, an expression reported by Tattitch and Blundy (2017) yielded a value of $D_{Mo}^{f/m}$ of 30.2 for conditions similar to those mentioned above for the $D_{Mo}^{s/m}$ value assumed from Fang and Audétat (2022). Using this value (30), the corresponding Mo concentration in the fluid would be 9,000 ppm Mo. The Mo concentrations estimated using partition coefficient of Fang and Audétat (2022) and Tattitch and Blundy (2017) therefore bracket the concentration of Mo estimated for the Preissac microgranite vug-filling fluid (7,800 ppm). Significantly, it is within the range of concentrations measured by Ulrich and Mavrogenes (2008) for the solubility of Mo in NaCl-bearing fluids (2,400 and 9,600 ppm) at a temperature and pH similar to those that might have prevailed in the Preissac microgranite (the pressure and fO_2 were likely lower); the concentration measured by Shang et al. (2020) at lower temperature (4,600 ppm) is also in this range.

IMPLICATIONS

Integrating data from the current study with the conceptual framework developed for the

evolutionary path of volatile-rich magmas by Whitney (1975), Shinohara et al. (1995), and Candela (1997), we propose the following model for the crystallization of the Preissac microgranite and the formation of the molybdenite-bearing vugs. A body of magma at a depth equivalent to a pressure of at least 3.5 Kbar fractionated into biotite-muscovite and muscovite monzogranites, which intruded overlying metavolcanic and sedimentary rocks. This left behind a small volume of highly evolved residual melt, which eventually was also expelled from the magma chamber and intruded zones of dilation in the muscovite monzogranite. The resulting reduction in pressure led to vesiculation or 'degassing' of the expelled magma and its consequent quenching to produce the fine-grained texture of the microgranite (see Jahns and Burnham, 1969; Webber et al., 1999; Zieg and Marsh, 2002). The expelled aqueous fluid pockets (bubbles) efficiently scavenged Mo, S and other elements from the magma but eventually were frozen *in situ,* probably while they were coalescing or *en route* to the zone of volatile accumulation. On subsequent cooling they precipitated molybdenite. The molybdenite-bearing vugs in the Preissac microgranite dikes therefore provide a rare record of the molybdenum concentration in an unevolved magmatic aqueous fluid that was deciphered from the volume proportion of molybdenite in the vugs.

ACKNOWLEDGEMENTS

Financial support for this study was provided by a grant from the National Sciences and Engineering Research Council of Canada to A.E.W-J. Larry Hoy of the Université de Montréal supervised the oxygen isotope analyses. Robert Marr assisted in sampling the vug-bearing microgranite. TM thanks Lee Groat of the University of British Columbia for a 2003 trip to the Little Nahanni pegmatite field, Northwest Territories, which fortuitously led to the recognition of

vesicle-laden basalt flows (Fig. 7) on the Yellowknife-Teslin highway, Yukon. We thank R. Seal II, P. Candela and D. Kontak for their inputs of an earlier version of the manuscript. Constructive comments by *American Mineralogist* referees, N.M and Bryan Maciag helped improve the manuscript substantially. Associate editor Julie Roberge and editorial staff are thanked for handling the submission and reviewing processes.

REFERENCES CITED

Anderko, A and Pitzer K.S. (1993) Equation of state representation of phase equilibria and volumetric properties of the system NaCl-H_2O above 573°K. Geochimica et Cosmochimica Acta, 57, 1657–1680.

Audétat, A. (2010) Source and evolution of molybdenum in the porphyry Mo(-Nb) deposit at Cave Peak. Texas. Journal of Petrology, 51, 1739–1760.

Audétat, A., and Pettke, T. (2003) The magmatic-hydrothermal evolution of two barren granites: A melt and fluid inclusion study of the Rito del Medio and Canada Pinabete plutons in northern New Mexico (USA). Geochimca et Cosmochimica Acta, 67, 97–121.

Audétat, A., Dolejs, D., and Lowenstern, J.B. (2011) Molybdenite saturationin silicic magmas: Occurrence and petrological implications. Journal of Petrology 52, 891–904.

Audétat, A., and Li, W. (2017) The genesis of Climax-type porphyry Mo deposits: insights from fluid inclusions and melt inclusions. Ore Geology Reviews, 88, 436–460.

Bai, T.B., and van Groos, A.F.K. (1999) The distribution of Na, K, Rb, Sr, Al, Ge, Cu, W, Mo, La, and Ce between granitic melts and coexisting aqueous fluids. Geochimica et Cosmochimica Acta, 63, 1117–1131.

Baker, J.H., Hellingwerf, R.H., and Hammergren, P. (1987) Geochemistry of a Proterozoic high silica W-Mo granite from Västra Gråshöjden, central Sweden: GeologiskaForeningensi Stockholm Forhandlinger, 109, 111–121.

Blevin, P., L., and Chappell, B.W. (1992) The role of magma sources, oxidation states and fractionation in determining the granite metallogeny of eastern Australia. Transactions of the Royal Society of Edinburgh: Earth Sciences, 83, 305–316.

Boynton, W.C. (1984) Cosmochemistry of the rare-earth elements: meteorite studies. In P. Henderson, Ed., p. 63–107, Rare Earth Element Geochemistry, Elsevier, Amsterdam.

Brown, W., and Parsons, I. (1989) Alkali feldspars: ordering states, phase transformations and behaviour diagrams for igneous rocks. Mineralogical Magazine, 53, 25–42.

Burnham, C.W. (1979) The importance of volatile constituents. InH.S. Yoder Jr. Ed.,The

Evolution of the Igneous Rocks, p.439–482. Princeton University Press, Princeton.

Candela, P.A. (1997) A review of shallow, ore-related granites: textures, volatiles, and ore metals. Journal of Petrology, 38, 1619–1633.

Candela, P.A. (1991) Physics of aqueous phase exsolution in plutonic environments. American Mineralogist, 76, 1081–1091.

Candela, P.A. (1992) Controls on ore metal ratios in granite-generated ore systems: an experimental and computational approach: Transactions of the Royal Society of Edinburgh: Earth Sciences, 83, 317–326.

Candela, P.A., and Belvin, P.L. (1995) Do some miarolitic granites preserve evidence of magmatic volatile phase permeability? Economic Geology, 90, 2310–2316.

Candela, P.A., and Holland, H.D. (1984) The partition of copper and molybdenum between silicate melts and aqueous fluids. Geochimica et Cosmochimica Acta, 48, 373–380.

Carten, R.B., Walker, B.M., Geraghty, E.P., and Gunow (1988) Comparison of field-based studies of the Henderson porphyry molybdenum deposit, Colorado, with experimental and theoretical models of porphyry systems. In R.P Taylor and D.F. Strong, Eds., Recent advances in the geology of granite-related mineral deposits, p. 351–366. The Canadian Institute of Mining and Metallurgy Special Volume 39.

Chakraborty, T., and Upadhyay, D. (2020) The geochemical differentiation of S-type pegmatites: constraints from major–trace element and Li–B isotopic composition of muscovite and tourmaline. Contributions to Mineralology and Petrology, 175**,** 60.

Chang, J., Li, J.W., and Zhou, L. (2020) Molybdenum isotopic fractionation in the Tibetan Yulong Cu-Mo deposit and its implications for mechanisms of molybdenite precipitation in porphyry ore systems. Ore Geology Reviews, 123, 103571.

Chevychelov, V., and Chcvychelova, T.K. (1997) Partitioning of Pb, Zn, W, Mo, CI, and major elements between aqueous fluid and melt in the systems granodiorite (granite, leucogranite)-H2O-NaCl-HCl. Neues Jahrbuchfür Mineralogie-Abhandlungen, 172, 101–115.

Clayton, R.N., and Mayeda, T.K. (1963) The use of bromine pentafluoride in the extraction of oxygen from oxides and silicates for isotopic analyses. Geochimica et Cosmochimica Acta, 27, 43–52.

Cline, J. S. and Bodnar, R.J. (1994) Direct evolution of brine from a crystallizing silicic melt at the Questa, New Mexico, molybdenum deposit. Economic Geology, 89, 1780–1802.

Congdon, R.D. and Nash, W.P. (1991) Eruptive pegmatite magma: rhyolite of the Honey Comb Hills, Utah. American Mineralogist, 76, 1261–1278.

Damman, A.H. (1989) The fluid evolution of a Proterozoic high-level anorogenic granite from the Gåsborn area, West Berslagen, central Sweden. Lithos, 22, 159–172.

Dawson, K.R. (1996) A comprehensive study of the Preissac-Lacorne Batholith, Abitibi County, Quebec. Geological Survey of Canada, Bulletin 142, 1966, 76 p.

Ducharme, Y., Stevenson, R., and Machado, N. (1997). Sm–Nd geochemistry and U–Pb geochronology of the Preissac and Lamotte leucogranites, Abitibi Subprovince. Canadian Journal of Earth Sciences, 34, 1059–1071.

Fang, J and Audétat, A. (2022) The effects of pressure, fO_2, fS_2 and melt composition on the fluid–melt partitioning of Mo: Implications for the Mo-mineralization potential of upper crustal granitic magmas. Geochimica et Cosmochimica Acta, 336, 1–14.

Farges, F., Siewert, R., Ponader, C. W., Brown, G. E., Pichavant, M., and Behrens, H. (2006) Structural environments around molybdenum in silicate glasses and melts. II. Effect of temperature, pressure, H_2O, halogens and sulfur. Canadian Mineralogist, 44, 755–773.

Greaney, A.T., Rudnick, R.L., Gaschnig, R.M., Whalen, J.B., Luais, B., and Clemens, J.D. (2018) Geochemistry of molybdenum in the continental crust. Geochimica et Cosmochimica Acta, 238, 36–54.

Hannah, J., Stein, H., Wieser, M.E., De Laeter, J.R., and Varner, M.D. (2007) Molybdenum isotope variations in molybdenite: Vapor transport and Rayleigh fractionation of Mo. Geology, 35, 703–706.

Hibbard, M.J.(1980) Indigenous Source of late-stage dikes and veins in granitic plutons. Economic Geology, 75, 410–423.

Hibbard, M.J., and Watters, R.J. (1985) Fracturing and diking in incompletely crystallized granitic plutons. Lithos, 18, 1–12.

Hoy, L.D. (1993) Regional evolution of hydrothermal fluids in the Noranda district, Quebec: evidence from $\delta^{18}O$ values from volcanogenic massive sulfide deposits. Economic Geology, 88, 1526–1541.

Jahns, R.H., and Burnham, W.C. (1969) Experimental studies of pegmatite genesis, I. A model for the derivation and crystallization of granitic pegmatites. Economic Geology, 64, 843–864.

Jian, W., Lehmann, B., Mao, J., Ye, H., Li, Z., He, H., Zhang, J., Zhang, H., and Feng, J. (2015) Mineralogy, Fluid Characteristics, and Re-Os Age of the Late TriassicDahu Au-Mo Deposit, Xiaoqinling Region, Central China: Evidence for a Magmatic-Hydrothermal Origin. Economic Geology, 110, 119–145.

Jiang, Z., Shang, L., Guo, H.,Wang, X-S., Chen, C., and Zhou, Y. (2021) An experimental in vestigation into the partition of Mo between aqueous fluids and felsic melts: Implications for the genesis of porphyry Mo ore deposits. Ore Geology Review, 134,104144.

Kaufmann, A.K.C., Pettke, T., and Wille, M. (2021) Molybdenum isotope fractionation at upper-crustal magmatic-hydrothermal conditions. Chemical Geology, 578, 120319.

King, P.L. and White, A.J.R. (2003) Granites, volatile solubility and tracking the formation of magmatic fluids. In P. Blevin, M. Jones and B. Chappell, Eds., Magmas to mineralization, The Ishihara Symposium, p. 85–88. Geoscience Australia, Record 2003/14.

Kirkham, R.V., McCann, C., Prasad, N., Soregaroli, A.E., Vokes, F.M. and Wine, G. (1982) Molybdenum deposits and occurrences in Canada. Geological Survey of Canada, Economic

Geology Report 33, 208 p.

Klemm,L.M, Pettke, T., and Heinrich, C.A. (2007) Hydrothermal evolution of the El Teniente deposit, Chile: Porphyry Cu-Mo ore deposition from low-salinity magmatic fluids: Economic Geology, 102, 1021–1045.

Kudrin, A.V. (1986) The solubility of tugarinovite MoS_2 in aqueous solutions at elevated temperatures. Geochemistry International, 22, 126–138.

Larsen, J.F., Denis, M-H., and Gardner, J.E. (2004).Experimental study of bubble coalescence in rhyolitic and phonolitic melts. Geochimica et Cosmochimica Acta, 68, 333–344.

Lerchbaumer, L., and Audétat, A. (2013) The metal content of silicate melts and aqueousfluids in subeconomically Mo-mineralized granites: implications for porphyry Mo genesis. Economic Geology, 108, 987–1013.

Monier, G., and Robert, J-L. (1986) Muscovite solid solutions in the system K_2O-MgO-FeO-Al_2O_3-SiO_2-H_2O: an experimental study at 2 kbar PH_2O and comparison with natural Li-free white micas. Mineralogical Magazine, 50, 257–266.

Mulja, T., Williams-Jones, A.E., Boily, M., and Wood, S.A. (1995a) The rare-element monzogranite-pegmatite systems in the Preissac-Lacorne batholith, Quebec: I. Geology and mineralogy. Canadian Mineralogist, 33, 793–832.

Mulja, T., Williams-Jones, A.E., Wood, S.A., Boily M. (1995b) The rare-element monzogranite-pegmatite systems in the Preissac-Lacorne batholith, Quebec: II. Geochemistry and Petrogenesis. Canadian Mineralogist, 33, 817–833.

Mutschler, F.E. Wright, E.G., Luddington, S., and Abbott, J.T. (1981) Granite molybdenite systems: Economic Geology, 76, 874–897.

Noble, D.C., Vogel, T.A., Peterson, P.S., Landis, G.P., Grant N.K.,Jezek, P.A. and McKee, E.H. (1984) Rare-element-enriched S-type ash-flow tuffs containing phenocrysts of muscovite, andalusite and sillimanite, Southeastern Peru. Geology, 12, 35–38.

Öhlander, B., Billström, K., and Hålenius, E. (1989) Behaviour of rare-earth elements in highly evolved granitic systems: evidence from Proterozoic molybdenite mineralized aplites and associated granites in northern Sweden. Lithos, 23, 267–280.

Ohmoto, H., and Rye, R.O. (1979) Isotopes of sulfur and carbon. In H.L. Barnes, Ed., Geochemistry of hydrothermal ore deposits, p.509–567. John Wiley& Sons, New York.

Pouchou, J.L. & Pichoir, F. (1984): A new model for quantitative X-ray microanalyses. Part I: application to the analysis of homogeneous samples. La Rech Aeros. 3, 13-38.

Rempel K. U., Migdisov A. A. and Williams-Jones A. E. (2006) The solubility of molybdenum in water vapour at elevated temperatures and pressures: implications for ore genesis. Geochimica et Cosmochimica Acta, 70, 687–696.

Peretyazhko, I.S., Zagorsky, V.Ye., Smirnov, S.Z., and Mikhailov, M.Y. (2005) Conditions of pocket formation in the Oktyabrskaya tourmaline-rich gem pegmatite (the Malkhan field, Central Transbailkalia, Russia). Chemical Geology, 210, 91–111.

Ross, P-S., Jébrak, M., and Walker, B.M. (2002) Discharge of hydrothermal fluids from a magma chamber and concomitant formation of a stratified breccia zone at the Questa porphyry molybdenum deposit, New Mexico. Economic Geology, 97, 1679–1699.

RyabchikovI.D., Rekharskiy V. I. and Kudrin A. V. (1981) Mobilization of molybdenum by fluids during the crystallizationof granite melts. Geochemistry International, 18,183–186.

Rudnick R. L. and Gao S. (2003) Composition of the continental crust. In R.L. Rudnick Ed., The Crust, p. 1–64. Elsevier-Pergamon, Oxford.

Rutherford MJ, Devine JD (1988) The May 18, 1980, eruption of Mount St. Helens 3. Stability and chemistry of amphibole in the magma chamber. Journal Geophysical Research, 93, 11949–11959.

Saleh, G.M. (2007) Geology and rare-earth element geochemistry of highly evolved, molybdenite-bearing granitic plutons, Southeastern Desert, Egypt. Chinese Journal of Geochemistry, 26, 333–344.

Schønwandt, H.K. (1988). Geology and geotectonic setting of cratonic porphyry molybdenum deposits in the North Atlantic region. In J. Boissonnas and P. Omenetto Eds., Mineral deposits within the European community, p. 210–229. Society for Geology Applied to Mineral Deposits Special Publication 6, Springer-Verlag, Berlin.

Shang, L., Williams-Jones, A.E., Wang, X., Timofeev, A., Hu, R., Bi, X. (2020) An experimental study of the solubility and speciation of MoO_3(s) in hydrothermal fluids at temperatures up to 350 °C. Economic Geology, 115, 661–669.

Shinohara, H., and Kazahaya, K. (1995) Degassing processes related to magma-chamber crystallization. In J.F.H. Thompson, Ed., Magmas, fluids, and ore deposits, p. 47–70. Mineralogical Association of Canada Short Course Series Volume 23.

Shinohara, H., Kazahaya, K., and Lowenstern, J.B. (1995) Volatile transport in a convecting magma column: implications for porphyry Mo mineralization. Geology, 23, 1091–1094.

Shvarov Y. and Bastrakov E. (1999)HCh: a software package for geochemical equilibrium modelling. User's guide: AustralianGeological Survey Organisation, Record 1999/25, 60 p.

Smith, R.W. (1983) Aqueous chemistry of molybdenum at elevated temperatures and pressures with applications to porphyry molybdenum deposits: unpublished Ph.D thesis, New Mexico Institute of Mining and Metallurgy, Socorro, NM., 311 p.

Štemprok, M. (1990) Solubility of tin, tungsten and molybdenum oxides in felsic magmas. Mineralium Deposita, 25, 212–225.

Stern, L.A., Brown Jr, G.E., Bird, D.K., Jahns, R.H., Foord, E.E., Shigley, J.E., and Spaulding Jr, L.B. (1986) Mineralogy and geochemical evolution of the Little Three pegmatite-aplite layered intrusive, Ramona, California. American Mineralogist, 71, 406–427.

Stein, H.J. (1988) Genetic traits of Climax-type granites and molybdenum mineralization, Colorado mineral belt. In R.P. Taylor and D.F. Strong, Eds., Recent advances in the geology of granite-related mineral deposits, p. 394–401. The Canadian Institute of Mining and Metallurgy

Special Volume 39.

Taner, H., Williams-Jones, A.E., and Wood, S.A. (1998) The nature and origin and physicochemical controls of hydrothermal Mo-Bi mineralization in the Cadillac deposit, Quebec, Canada. Mineralium Deposita, 33, 579–590.

Tattitch, B.C. and Blundy, J.D. (2017) Cu-Mo partitioning between felsic melts and saline-aqueous fluids as a function of X_{NaCleq}, f_{O2}, and f_{S2}. American Mineralogist, 102, 1987–2006.

Taylor, B.E., Foord, EE., and Friedrichsen, H. (1979) Stable isotope and fluid inclusion studies of gem-bearing granitic pegmatite-aplite dikes, San Diego County, California. Contributions to Mineralogy and Petrology, 68, 187–205.

Ulrich, T and Mavrogenes (2008) An experimental study of the solubility of molybdenumin H_2O and KCl–H_2O solutions from 500° C to 800° C, and 150 to 300 MPa. Geochimica et Cosmochimica Acta, 72, 2316–2330.

Villaros, A., Stevens, G., and Buick, I.S. (2009) Tracking S-type granite from source to emplacement: clues from garnet in Cape Granite suite. Lithos, 112, 217–235

Watt, P.D., 1967, Preissac molybdenite mines Ltd., Canadian Institute of Mining and Metallurgy field excursion guide book—northwest Quebec-northeast Ontario, p. 31–33.

Webber, K.L., Simmons, W.B., Falster, A.U., and Foord, E.E. (1999) Cooling rates and crystallization dynamics of shallow level pegmatite-aplite dikes, San Diego County, California. American Mineralogist, 84, 708–717.

Webster, J.D. (1997) Exsolution of magmatic volatile phases from Cl-enriched mineralizing granitic magmas and implications for ore metal transport. Geochimica et Cosmochimica Acta, 61, 1017–1029.

Webster, J.D., Thomas, R., Foster, H-J., Seltmann, R., and Tappen, C. (2004) Geochemical evolution of halogen-enriched granite magmas and mineralizing fluids of the Zinnwald tin-tungsten mining district, Erzgebirge, Germany. Mineralium Deposita, 39, 452–473.

Wedepohl, K.H. (1969) Handbook of Geochemistry, New York, Springer.

Wedepohl, K.H. (1995) The composition of the continental crust. Geochimica et Cosmochimica Acta, 59, 1217–1239.

Westra, G., and Keith, S.B. (1981) Classification and genesis of stockwork molybdenum deposits.Economic Geology, 76, 844–873.

Whitney, J.A. (1975) Vapor generation in a quartz monzonite magma: a synthetic model with application to porphyry copper deposits. Economic Geology, 70, 346–358.

Williams-Jones, A.E., and Heinrich, C.A. (2005) Vapor transport of metals and the formation of magmatic-hydrothermal ore deposits. Economic Geology, 100, 1287–1312.

Zajacz Z., Candela P.A., and Piccoli P.M. (2017) The partitioningof Cu, Au and Mo between liquid and vapor at magmatic temperatures and its implications for the genesis of magmatic hydrothermal ore deposits. Geochimimica et Cosmochimica Acta, 207, 81–101.

Zajacz, Z., Halter, W.E., Pettke, T., and Guillong, M. (2008) Determination offluid/melt partition

coefficients by LA-ICPMS analysis of co-existing fluid and silicate melt inclusions: controls on element partitioning. Geochimica et Cosmochimica Acta, 72, 2169–2197.

Zieg, M.J., and Marsh, B.D. (2002) Crystal size distributions and scaling laws in the quantification of igneous textures. Journal of Petrology, 43, 85–101.

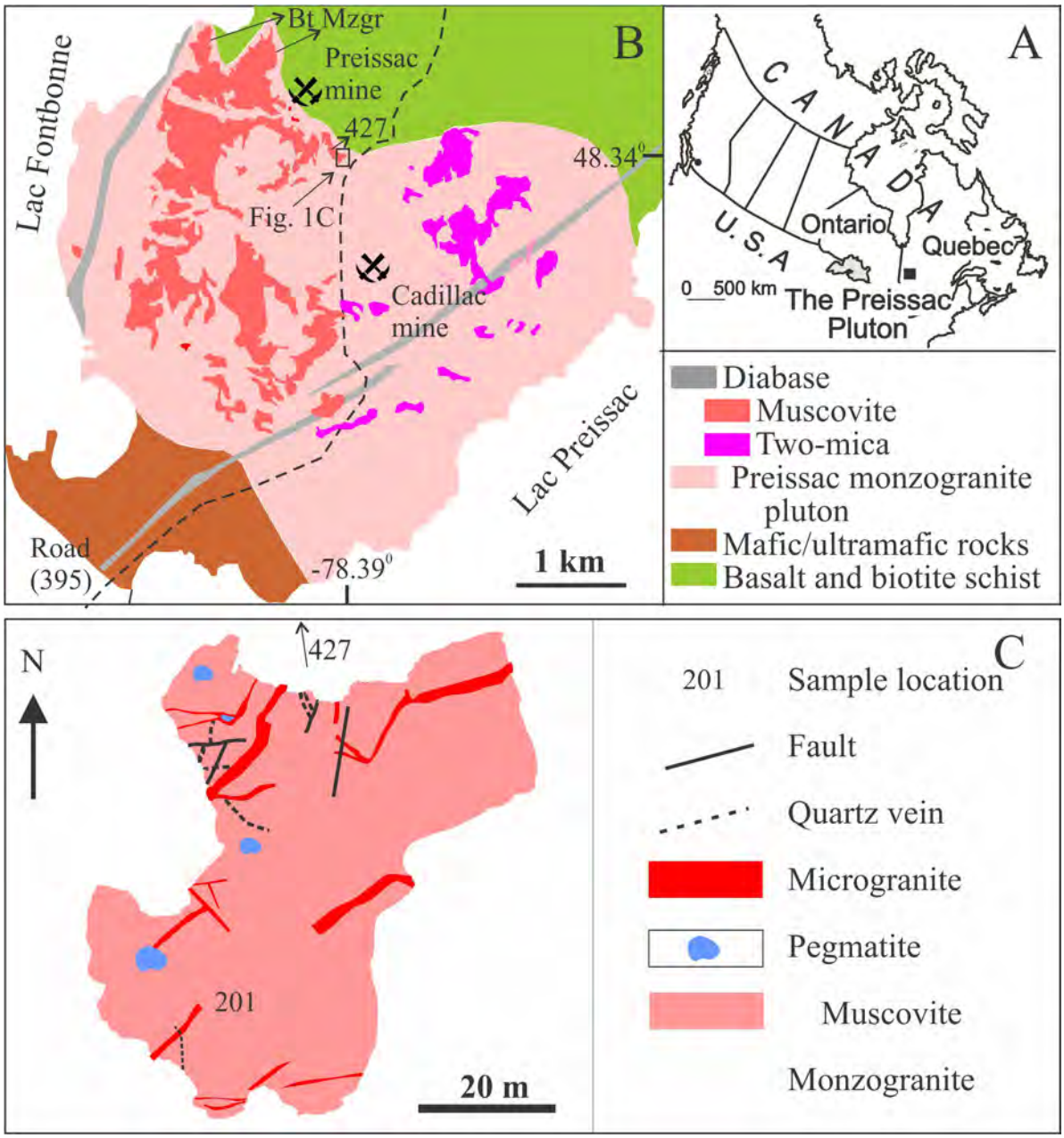

1. A. A location map forthe Preissac pluton in western Québec.
   B. A geological map of the Preissac pluton showing the location of the microgranite dikes with respect to other granitic rocks (Dawson, 1996; Mulja et al. 1995a; this study). Bt Mzgr: biotite monzogranite.
   C. The distribution of microgranite dikes in the muscovite monzogranite. Samples 471, 3, 7, 9 are located near sample 201.

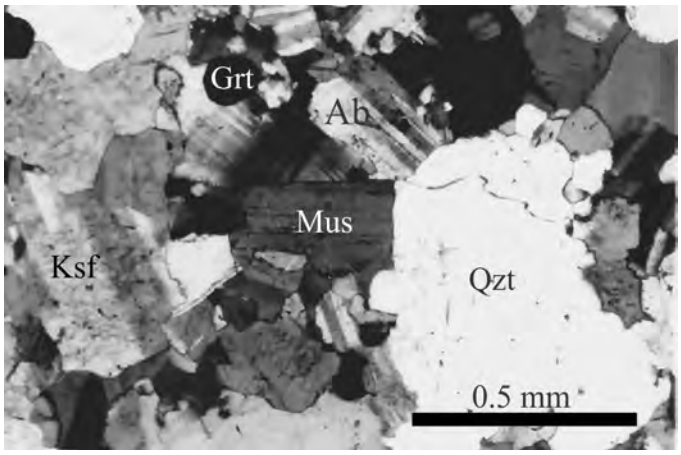

2. A cross-polarized photomicrograph of the microgranite showing interlocking crystals of quartz (Qzt), potassium feldspar (Ksf), albite (Ab), and muscovite (Mus). Note that the muscovite crystals are similar in size to those of the albite and K-feldspar. Garnet (Grt) appears as optically extinct sub-rounded crystals.

This is the peer-reviewed, final accepted version for American Mineralogist, published by the Mineralogical Society of America.
The published version is subject to change. Cite as Authors (Year) Title. American Mineralogist, in press.
DOI: https://doi.org/10.2138/am-2022-8770. http://www.minsocam.org/

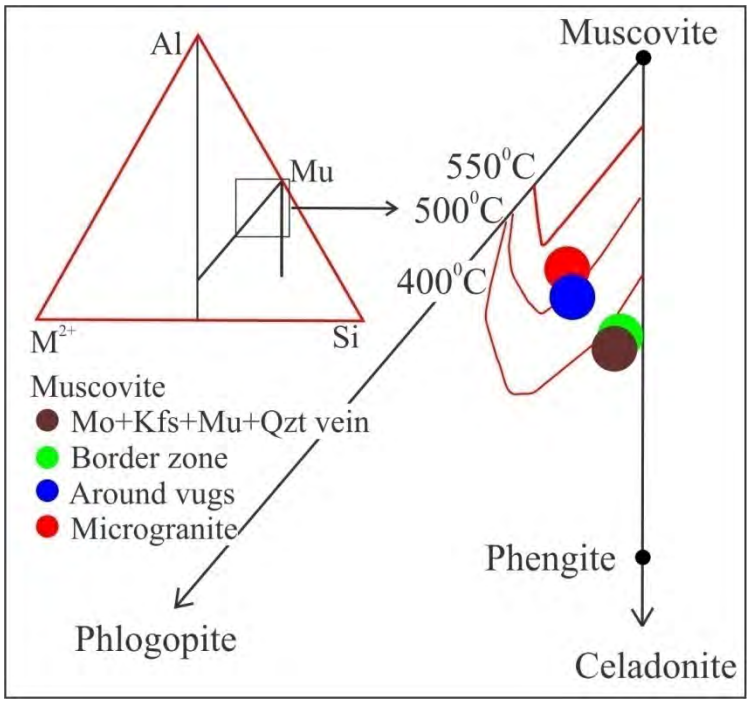

3. Average compositions of muscovite in various parageneses as atomic proportions of M^{2+}(Fe + Mg + Mn)–Si–ΣAl together with isotherms experimentally determined for 300° to 700° C and 2 kbar P_{H_2O} showing the corresponding formation temperatures (after Monier and Robert, 1986).

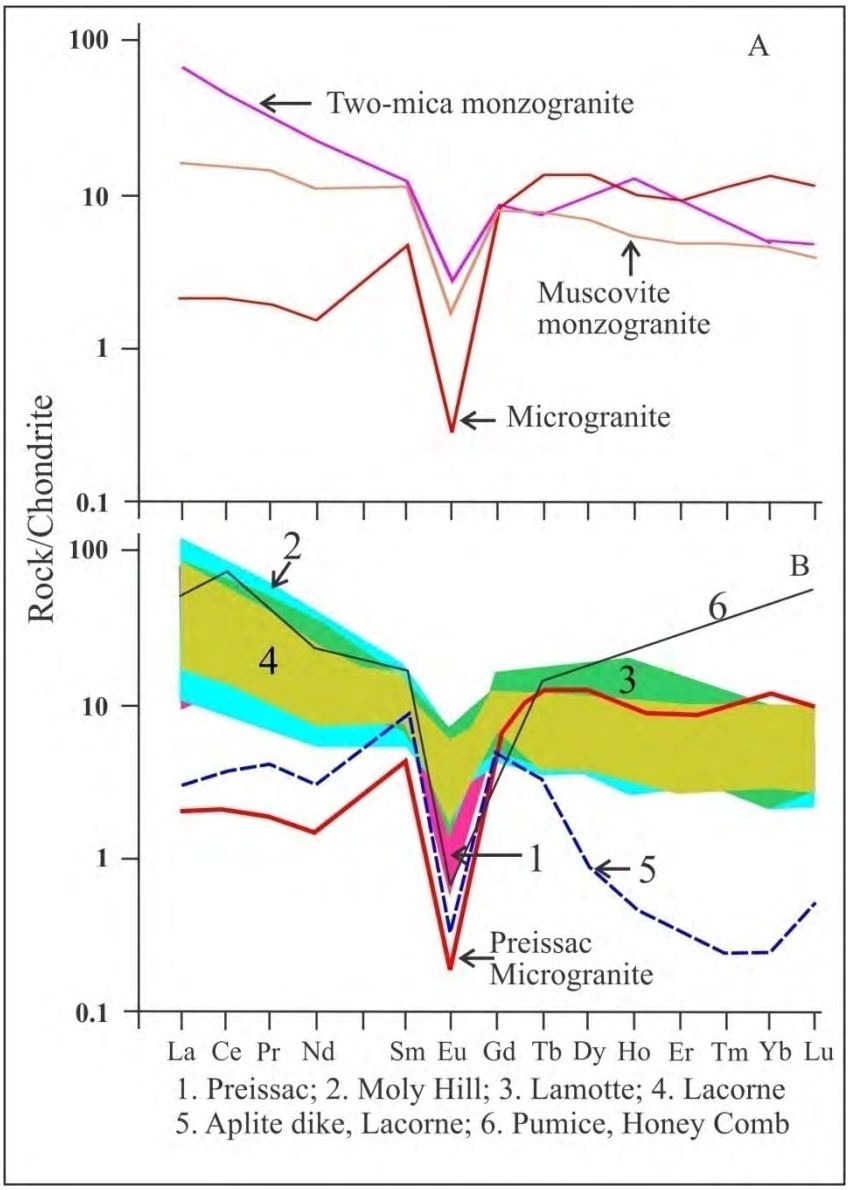

4. A. Chondrite-normalized REE (REE_N) profiles for the microgranite and associated monzogranites in the Preissac pluton, indicating that the microgranite is the most evolved of the three granite types (after Mulja et al., 1995b). The normalizing values are from Boynton (1984).

   B. A comparison of thechondrite-normalized REE_N profile for the microgranite with those forthe Preissac-Lacorne monzogranites and for the REE_N profile of the most evolved pumice from the Honey Comb rhyolite (number 6), which is considered to be an equivalent of eruptive pegmatites (Congdon and Nash, 1991). The data for the Preissac-Lacorne samples are from Mulja et al. (1995b).

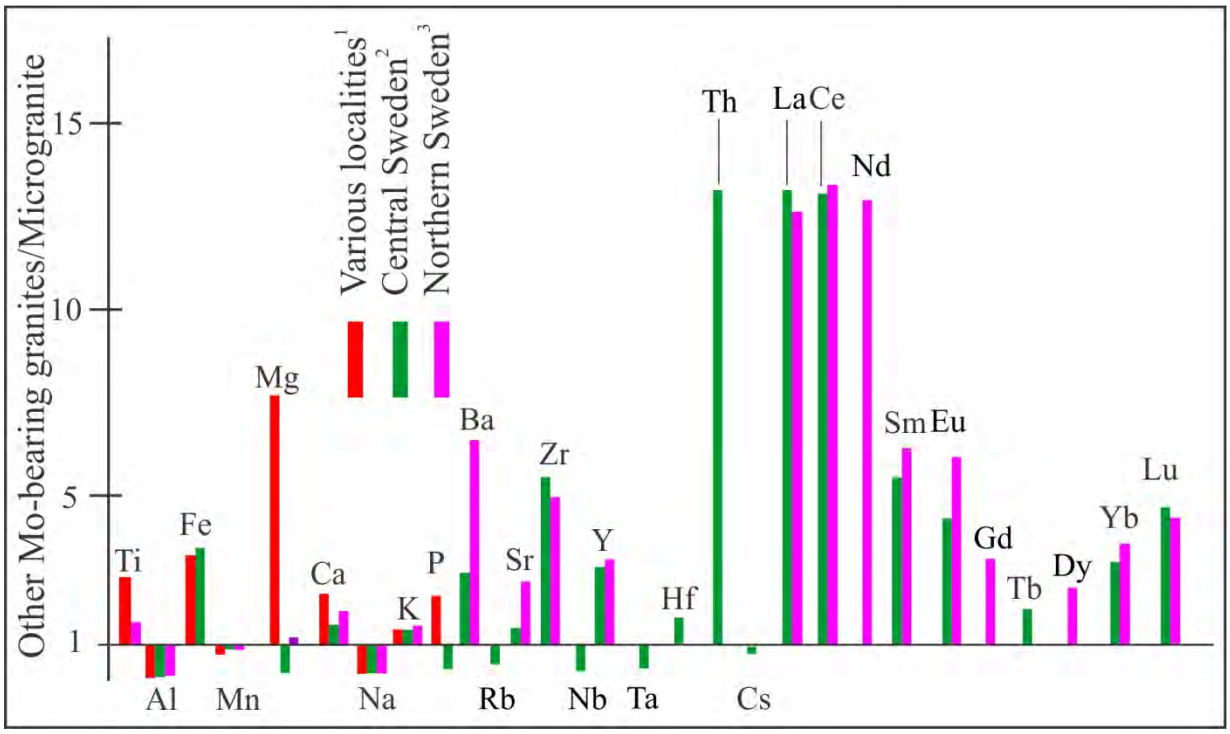

5. The trace and rare-earth element concentrations of selected Mo-related granites normalized to those of the Preissac microgranite. Sources of information: 1. Mutschler et al. (1981); 2. Central Sweden, samples 7798006 & 0539108, Baker et al. (1987); 3. Öhlander et al. (1989). The normalizing composition of the microgranite is from Mulja et al. (1995b).

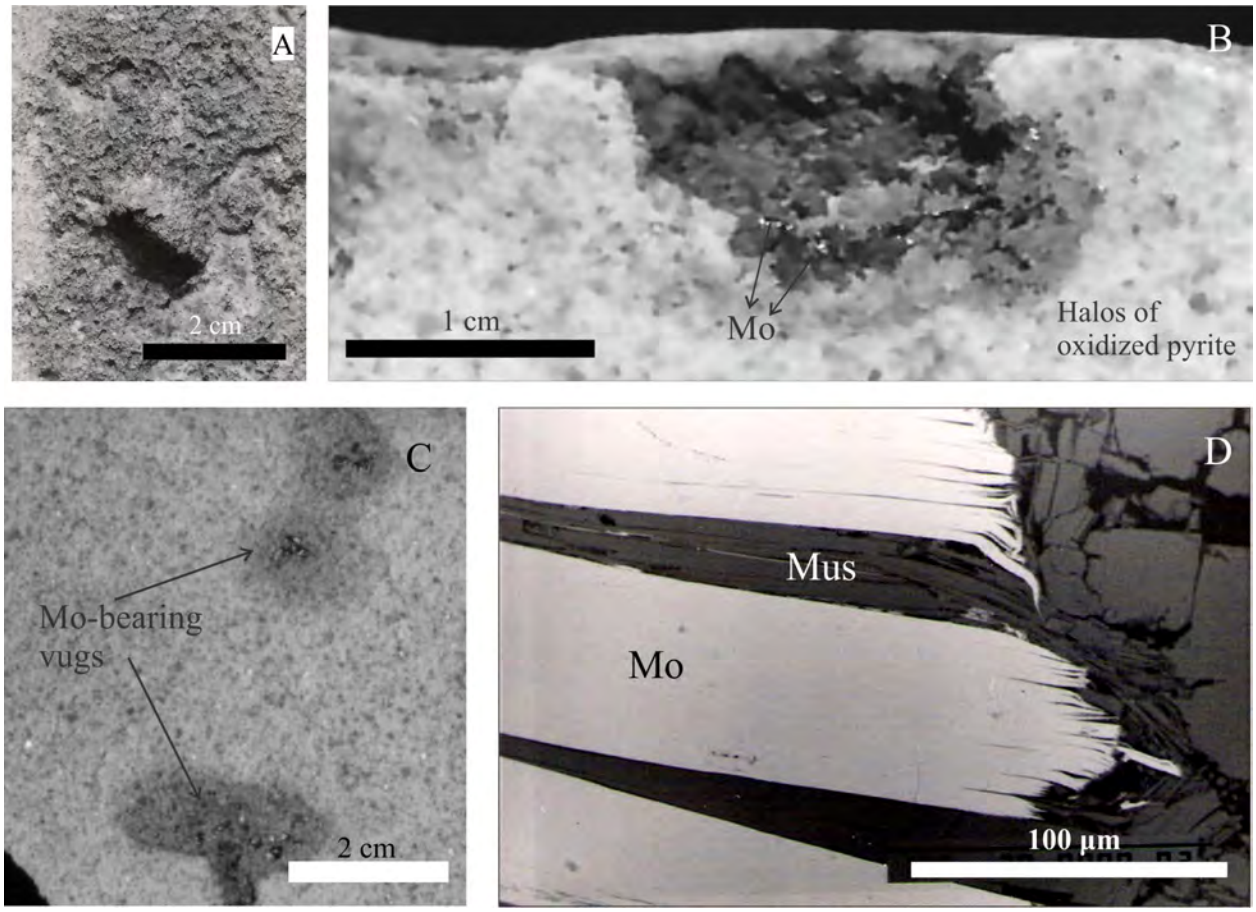

6. A. A molybdenite-bearing vug in the microgranite as seen from above.
   B. The molybenite (Mo) vug in A shown in cross section.
   C. A string of Mo-bearing vugs in a cross-section of a microgranite slab.
   D. Interstitial muscovite between molybdenite blades in a vug.

7. Vesicle columns in basaltic lava flows in a roadcut on the Yellowknife – Teslin highway in Yukon, Canada (photographed by D. Kontak). The vugs in the monzogranite may represent vesicles in columns analogous to those whichit is proposed formed during exsolution of fluid from the Preissac microgranite-forming magma. Note that the height of bubble nucleation varied and that some bubbles ceased migrating within the flow (left bottom), whereas others reached the top of a flow unit or a fracture plane, spread laterally and probably coalesced to form a zone or zones of high volatile concentration. The pen is approximately 13 cm long.

This is the peer-reviewed, final accepted version for American Mineralogist, published by the Mineralogical Society of America.
The published version is subject to change. Cite as Authors (Year) Title. American Mineralogist, in press.
DOI: https://doi.org/10.2138/am-2022-8770. http://www.minsocam.org/

Table 1. Average compositions of feldspars, muscovite and garnet from the Preissac microgranite, vugs and vein

Host	1	1	2	2	3	3
N	8*	6*	3	2	4	2
-	Plag	Ksf	Plag	Ksf	Plag	Ksf
SiO_2	67.8	64.2	68.2	65.4	69.0	64.6
Al_2O_3	20.0	18.2	20.1	17.9	19.6	18.4
Na_2O	11.0	0.44	11.2	0.52	11.6	0.66
K_2O	0.1	16.9	0.1	16.6	0.11	16.4
CaO	0.71	0.02	1.0		0.16	
Total	99.5	99.8	99.5	99.5	100.5	100.1
Si	2.9728	2.9856	2.9670	3.0141	2.9964	2.9902
Al	1.0317	1.0007	1.0287	0.9710	1.0042	1.0029
Na	0.9369	0.0397	0.9465	0.1646	0.9744	0.0588
K	0.0033	1.0035	0.0042	0.9750	0.0059	0.9686
Ca	0.0331	0.0003	0.0455		0.0073	
Ab	96.2	3.81	95.0	4.53	98.7	5.72
Or	0.34	96.2	0.43	95.5	0.60	94.3
An	3.42	0.0	4.57		1.21	

	1	2	3	4
	11*	5	4	4
	Muscovite			
SiO_2	45.9	46.6	47.7	47.5
TiO_2	0.18	0.23	0.22	0.69
Al_2O_3	31.6	30.9	31.2	29.4
FeO	5.28	5.60	4.14	3.78
MnO	0.14	0.11	0.06	0.10
MgO	0.42	0.55	1.29	1.54
Na_2O	0.29	0.25	0.32	0.52
K_2O	11.2	11.0	11.1	11.5
F			0.8	
Total	95.0	95.2	96.0	95.0
Si	6.2893	6.3661	6.5670	6.4978
Ti	0.0185	0.0238	0.0103	0.0677
^{iv}Al	1.7107	1.6339	1.4330	1.5022
^{vi}Al	3.3910	3.3427	3.3643	3.2212
ΣAl	5.1017	4.9766	4.7973	4.7234
Fe	0.6060	0.6399	0.3288	0.4218
Mn	0.0161	0.0126	0.0060	0.0139
Mg	0.0850	0.1118	0.3442	0.2902
ΣM^{2+}	0.7072	0.7643	0.6730	0.7259
Na	0.0764	0.0661	0.0630	0.0707
K	1.9590	1.9132	1.8870	2.0413

	1
	21*
	Garnet
SiO_2	36.0
TiO_2	0.13
Al_2O_3	19.7
Fe_2O_3	1.16
FeO	16.4
MnO	25.4
MgO	0.19
CaO	0.74
Total	99.8
Si	5.9894
Ti	0.0298
^{iv}Al	0.0377
Fe^{3+}	0.1411
^{vi}Al	3.8432
Fe^{2+}	2.2999
Mn	3.5806
Mg	0.0713
Ca	0.1350
Alm	37.8
Prp	0.80
Grs	0
Sps	59.2
Adr	2.18

*two analyses were published in Mulja (1995a)

Host: 1: Microgranite at various distances from the Mo-bearing vugs
2: Around and in the Mo-bearing vugs
3. Monzogranite bordering with the Preissac Mo+Kfs+Mu quartz vein (host No. 4)
4: Preissac Mo quartz vein ore.

N: number of analyses

Number of cations is on the basis of 6 (feldspars), 22 (muscovite) and 24 (garnet) atoms.

This is the peer-reviewed, final accepted version for American Mineralogist, published by the Mineralogical Society of America.
The published version is subject to change. Cite as Authors (Year) Title. American Mineralogist, in press.
DOI: https://doi.org/10.2138/am-2022-8770. http://www.minsocam.org/

Table 2. Geochemisry of muscovite-garnet microgranite of the Preissac pluton *

Major elements (wt.%)	n = 2	Trace elements (ppm)	n = 1 or 2	Rare-earth element	n = 1
SiO_2	75.8	Ba	4.62 (1)	La	0.64
TiO_2	0.02	Rb	472 (2)	Ce	1.67
Al_2O_3	14.5	Sr	7.81 (2)	Pr	0.23
Fe_2O_3(t)	0.43	Zr	16.2 (2)	Nd	0.90
MnO	0.26	Nb	73 (2)	Sm	0.88
MgO	0.06	Y	24.2 2)	Eu	0.02
CaO	0.31	Ta	7.22 (1)	Gd	2.08
Na_2O	4.82	Hf	2.97 (1)	Tb	0.62
K_2O	3.65	Th	1.36 (1)	Dy	4.22
P_2O_5	0.04	U	2.39 (1)	Ho	0.70
L.O.I	0.42	Cs	16.8 (1)	Er	1.87
Total	100.3	Sc	2.18 (1)	Tm	0.35
		Cu	6.95 (1)	Yb	2.70
A/CNK: 1.2		Pb	18 (1)	Lu	0.36
		Zn	13.8 (1)		
		Mo	0.35 (1)	ΣREE	17.24

*Partially published in Mulja et al. (1995b)